Topological evolution of self-induced silicon nanogratings during prolonged femtosecond laser irradiation

E.V. Golosov · A.A. Ionin · Y.R. Kolobov · S.I. Kudryashov · A.E. Ligachev · S.V. Makarov · Y.N. Novoselov · L.V. Seleznev · D.V. Sinitsyn

Abstract Gradual evolution of self-induced silicon surface topology from one-dimensional ridge-like to two-dimensional spike-like nanogratings and then to isotropic sets of micro-columns was observed by evenly increasing IR and UV femtosecond laser irradiation dose. This topological evolution exhibits clear indications of consequent melting and vaporization processes being set up during the prolonged laser irradiation. Monotonously decreasing cumulative IR and UV femtosecond laser-nanostructuring thresholds may indicate an increase of optical absorbance of the laser-nanostructured silicon surfaces versus the increasing laser dose, consistent with the consequent onset of the abovementioned thermal modification processes.

1 Introduction

Femtosecond (fs) laser nano- and microstructuring of silicon surfaces appears as a promising way in fabricating highly sensitive silicon substrates for surface-enhanced Raman scattering (SERS) [1, 2] and strongly absorbing silicon photodetectors [3, 4], with their unique optical characteristics provided by isotropic arrays of nano-spikes and micro-columns [1–4], respectively. Although technological perspectives of the fs-laser surface modification technique in fabricating such nano- and microstructured silicon devices are quite distinct, clear understanding of the underlying fundamental physical nano- and microstructuring mechanisms, involving effects of laser polarization (vector **e**), wavelength λ and pulse duration τ, laser fluence F, and the number of incident pulses N on topologies and other physical or chemical characteristics, as well as transient dynamics of the resulting surface nano- and microstructures is still missing, despite of the related material science studies [1–8]. Ablative Coulomb explosion [5], melting accompanied by vaporization [6, 7], or purely thermal melt instabilities [8] suggested as potential mechanisms to explain fabrication of such surface structures appear to be too controversial and not well-evidenced to provide a clear physical picture of the surface nano- and microstructuring processes.

In this work, using SEM to visualize a surface nanorelief we tracked an effect of the fs-laser irradiation dose (the laser fluence F times the number of incident pulses N) on topologies of self-induced nanostructures and on nanostructuring thresholds for silicon surfaces irradiated by IR and UV fs-laser pulses, and interpreted the observed cumulative nanorelief evolution in terms of microscopic physical processes of nano- and micro-scale surface modification.

2 Experimental setup and techniques

The experiments were performed on an experimental setup including a Ti:Sa laser (Avesta Project) providing either first-harmonic pulses (central wavelength of 744 nm, FWHM parameter of 13 nm) with a duration of 80 fs (FWHM) and

E.V. Golosov · Y.R. Kolobov
Belgorod State University, Belgorod, Russia

A.A. Ionin · S.I. Kudryashov (✉) · S.V. Makarov · Y.N. Novoselov · L.V. Seleznev · D.V. Sinitsyn
P.N. Lebedev Physical Institute, Russian Academy of Sciences, 119991 Moscow, Russia
e-mail: sikudr@sci.lebedev.ru
Fax: +7-499-7833690

A.E. Ligachev
A.M. Prokhorov General Physics Institute, Moscow, Russia

S.V. Makarov
National Research Nuclear University "MEPHI", Moscow, Russia

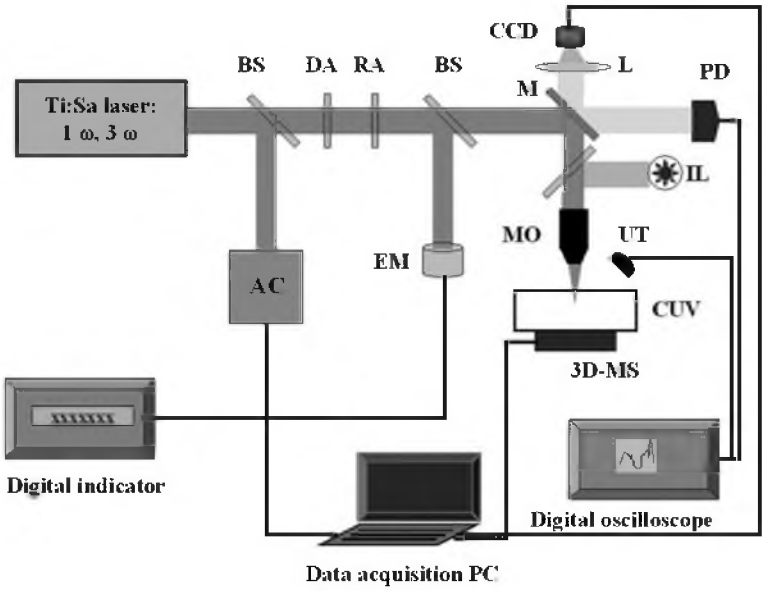

Fig. 1 Experimental setup for femtosecond laser surface nanostructuring of solids: BS—beam splitter, AC—autocorrelator, DA, RA—variable diffractive and reflective energy attenuators, EM—thermocouple energy meter, M—mirror, L—focusing fused silica lens, CCD—charge-coupled device camera for surface imaging, PD—fast trigger silicon photodiode, IL—illumination lamp, FL—focusing lens, UT—ultrasonic transducer, CUV—glass cuvette with the silicon sample for optional dry or wet nano- and microstructuring, 3D-MS—three-dimensional motorized micro-stage

an energy up to 8 mJ, or frequency-tripled pulses (central wavelength of 248 nm, FWHM parameter of 1.5 nm) with a duration of about 60 fs (FWHM) and an energy up to 0.5 mJ [9]. The transverse spatial distribution of such IR and UV fs-laser pulses corresponded to the TEM_{00} mode. The normally incident IR and UV laser pulses were weakly focused on a spot with a diameter about 0.3 mm (at a level of $1/e$) on the surface of a target [commercial undoped silicon Si(100) wafers] (Fig. 1). The target was placed onto a computer-controlled three-dimensional motorized stage. IR laser pulse energies were varied in the range of 6–100% by a reflective polarization attenuator (Avesta Project) and controlled by either a pyroelectric energymeter (OPHIR), or a calibrated photodiode DET-210 (Thorlab) illuminated by a weak laser beam split through a steering dielectric mirror. In the case of UV fs-laser pulses, their energy attenuation was performed in the range 4–100% by means of a diffractive micro-optical fused silica attenuator (Institute of Automatics and Electrometry, SB RAS) and was controlled using another calibrated DET-210 photodiode.

The nanostructuring experiments were performed by irradiating different circular spots of the stationary silicon target surface in ambient air by the different number of laser pulses $N = 100$, 300 and 1000 at rather low IR and UV fs-laser pulse energies (<0.3 mJ, peak power $W < 4$–5 GW) in order to avoid a noticeable degradation of the fluence distribution on the target surface because of their self-focusing in air and air plasma defocusing, as well as accompanying effects of chromatic emission, filamentation, and scattering on a plasma [10, 11]. Topological characterization of the resulting fs-laser fabricated nano- and micro-scale surface structures was performed by means of a scanning electronic microscope (SEM) Quanta FEG at magnifications up to 200 000×.

3 Experimental results

The SEM images of the UV fs-laser-nanostructured silicon surface spots demonstrated at $F \approx 0.09$ J/cm^2 and $N \approx 100$ pulses well-defined one-dimensional nanogratings (Fig. 2a) with periods $\Lambda \approx 0.5$ μm oriented perpendicularly to the polarization of the laser electric field **e** (grating wavevector $\mathbf{q} \| \mathbf{e}$), as typical for the well-known "interference" fabrication mechanism, according to Sipe et al. [12] and Akhmanov et al. [13]. Similarly, the SEM image of such nanogratings yields in a rather simple two-dimensional fast Fourier transform (FFT) spectrum (Fig. 2d) indicating their regular one-dimensional character evidenced by the symmetrical lateral features in the spectrum.

At higher irradiation dose ($F \approx 0.09$ J/cm^2, $N \approx 300$ pulses) the regular nanogratings become damaged via breaking of their ridges (Fig. 2b), represented by significant reduction of intensity for the lateral features in the corresponding FFT spectrum and the simultaneous intensity rise for the isotropic component (central bright spot in Fig. 2e). The closer, high-magnification view at the breaking points (Fig. 3a) showed a number of round-shaped fragments and droplet-like spikes indicating that the instability of the gratings resulted from displacement of molten fragments of the gratings, potentially, via nano-scale capillary effects. Moreover, the transverse nano-pores between the nano-spikes clearly visible in Fig. 3a on its right side, but not very pronounced in the FFT spectrum in Fig. 2e, demonstrated a double period ≈1 μm.

Finally, at the maximum laser irradiation dose ($F \approx 0.09$ J/cm^2, $N \approx 10^3$ pulses) the grating-like structure completely disappeared on the surface topology (Fig. 2c), resulting via the abovementioned breakage process in an isotropic set of micro-columns, as shown in the corresponding FFT

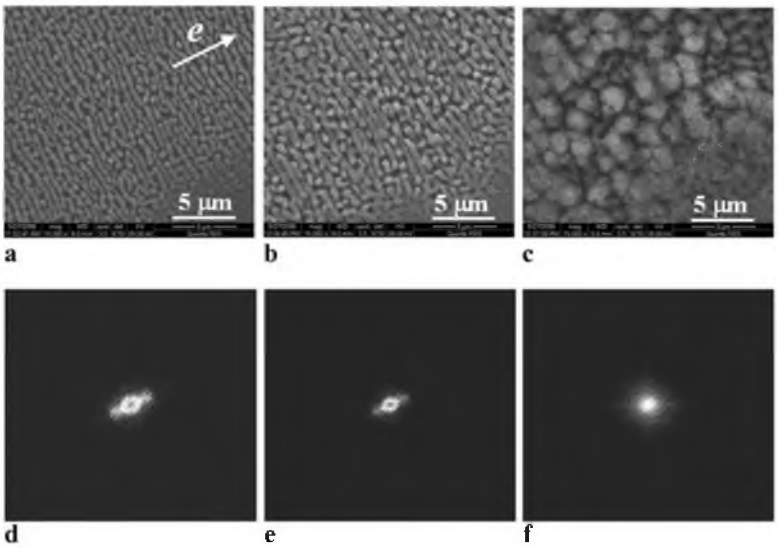

Fig. 2 Low-magnification SEM images of Si surface nanostructured in air by UV fs-laser pulses at $F \approx 0.09$ J/cm^2 and $N \approx 100$ (**a**), 300 (**b**) and 1×10^3 (**c**) pulses, and their corresponding FFT spectra (**d–f**)

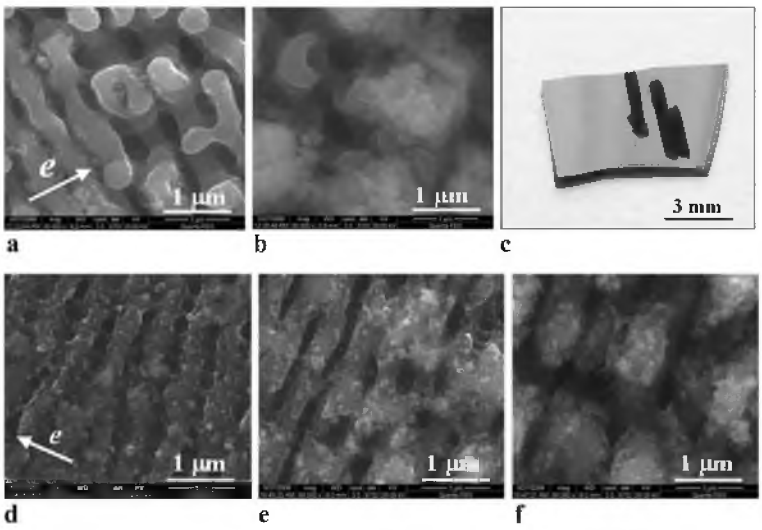

Fig. 3 High-magnification SEM image of Si surface nanostructured in air by UV ((**a–b**), $F \approx 0.09$ J/cm^2) and IR ((**d–f**), $F \approx 0.2$ J/cm^2) fs-laser pulses for $N \approx 100$ (**d**), 300 (**a**, **e**), or 1×10^3 (**b**, **f**) pulses, respectively. (**c**) Optical image of the highly absorbing fs-laser-nanostructured "*black*" *region* on the silicon wafer (image size 3×3 mm)

spectrum in Fig. 2f. These micro-columns exhibited a significant amount of amorphous silicon flakes resided on them due to the intense vaporization (boiling) and re-deposition processes (Fig. 3b).

Likewise, the IR fs-laser silicon surface spots nanostructured at $F \approx 0.2$ J/cm^2 and $N \approx 100$ or 300 pulses demonstrated well-defined or considerably degraded one-dimensional gratings with the typical periods $\Lambda \approx 0.5$ μm[1] oriented perpendicularly to the polarization of the laser (SEM images (d, e) in Fig. 3 and (a–b, d–e) in Fig. 4, respectively) while at higher $N \approx 10^3$ pulses such gratings were almost completely corrupted revealing presumably an isotropic distribution of micro-columns (image (f) in Fig. 3 and images (c, f) in Fig. 4). Again, at higher N we observed clear indications of melting of the grating ridges and the following merging between neighboring ones, finally resulting in rather isotropic sets of micro-columns covered by amorphous residue (Figs. 3f and 4c, f).

4 Discussion and conclusions

The striking similarities observed in this work between results of these IR and UV studies indicate the rather universal character of the observed nano- and micro-scale surface topology evolutions versus the IR and UV laser irradiation doses, going through a highly ordered one-dimensional ridge-like nanograting structure to partially and completely disordered two-dimensional spike-like ones.

The transformations of the silicon surface nano-topology observed versus increasing fs-laser irradiation dose occur at higher and higher surface temperatures, consequently

[1]The similarity of periods for silicon surface nanograting fabricated using the 248-nm and 744-nm fs-laser will be discussed in our next publications.

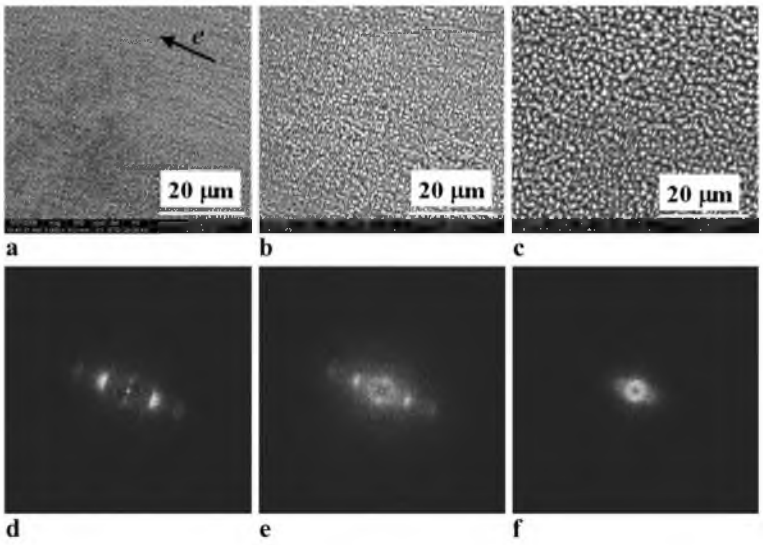

Fig. 4 Low-magnification SEM images of Si surface nanostructured in air by IR fs-laser pulses at $F \approx 0.2$ J/cm^2 and $N \approx 100$ (**a**), 300 (**b**) and 1×10^3 pulses (**c**), and their corresponding FFT spectra (**d**–**f**)

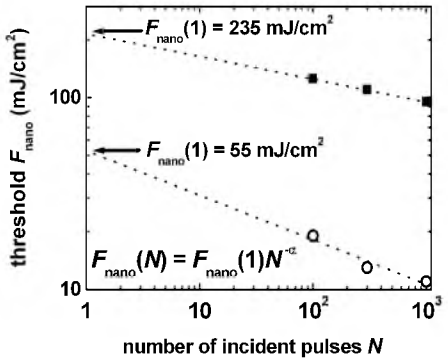

Fig. 5 Cumulative IR (*dark squares*) and UV (*light circles*) fs-laser surface nanostructuring thresholds $F_{\text{nano}}(N)$ for silicon versus N extrapolated to the single-shot thresholds $F_{\text{nano}}(N = 1)$ using the widely accepted expression, $F_{\text{nano}}(N) = F_{\text{nano}}(1)N^{-\alpha}$, for the cumulative material modification by laser radiation. The estimated IR single-shot threshold (235 mJ/cm^2) is reasonably close to the single-shot thermal melting threshold of silicon under similar conditions (0.2–0.25 J/cm^2 [14]), while for the UV fs-laser pulses there are no reference data

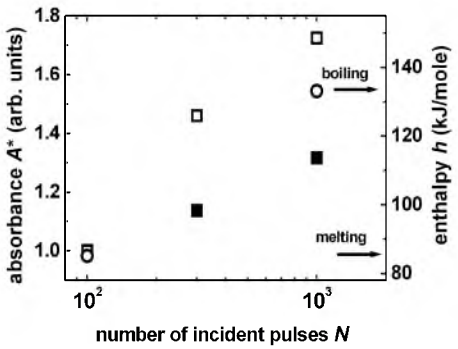

Fig. 6 Evaluated increase of optical absorbance $A^*(N)$ versus N for IR and UV fs-laser pulses (*left scale*, *dark* and *light squares*, respectively) and deposited surface enthalpy h (*right scale*) with *the two light circles* showing the melting point ($h_{\text{melt}} \approx 85$ kJ/mole [15]) and boiling point ($h_{\text{boil}} \approx 133$ kJ/mole [15]) enthalpy magnitudes for silicon

involving melting and vaporization processes. Since during the nano- and microstructuring processes the modified silicon surface finally results in a strongly absorbing silicon "black" ("black silicon" [6, 7, 16]) (see, for example, Fig. 3c), one may expect that it is the rising optical absorbance A of the gradually developing surface nano- and micro-relief that promotes the rising surface temperatures at the constant incident laser fluence. In support of this assumption we experimentally demonstrate the cumulative drop of the IR and UV fs-laser surface nanostructuring thresholds $F_{\text{nano}}(N)$ for silicon (Fig. 5) obtained via measurements of spatial dimensions for the nanostructured silicon surface spots as a function of IR or UV fs-laser energy. Such drop of the nanostructuring threshold versus increasing N and surface nanorelief can be reasonably considered in terms of increasing effective surface optical absorbance $A^*(N)$ [6, 17], overall providing the same effective (absorbed) surface fluence $A^*(N)F_{\text{nano}}(N) \approx$ constant, i.e., $A^*(N) \approx \text{constant}/F_{\text{nano}}(N)$. The estimated cumulative increase of $A^*(N)$ for the nanostructured silicon surfaces by 35–70% for N changing from 10^2 till 10^3 pulses (Fig. 6) reasonably agree with the experimentally observed transition from the presumable melting to the boiling of the molten material in the surface nanostructures with the two abovementioned thermal processes, characterized by the enthalpies $h_{\text{melt}} \approx 85$ kJ/mole and $h_{\text{boil}} \approx 133$ kJ/mole [14], and the same ratio of the enthalpies $h_{\text{boil}}/h_{\text{melt}} \approx 1.5$–$1.6$ (Fig. 6). The demonstrated consequence of the melting and boiling processes, setting up versus increasing fs-laser irradiation dose, is supported by previous assumptions on the ns laser-induced formation mechanism for silicon microcolumns [6, 7].

In conclusion, in this study we have experimentally identified basic physical–optical and thermal—processes underlying destructive evolution of IR and UV femtosecond

laser self-fabricated nanostructures on silicon wafer surfaces starting from regular one-dimensional nanogratings, finally, to isotropic sets of micro-columns.

Acknowledgements This work was supported by the Russian Foundation for Basic Research (project Nos. 08-08-00756a, 09-02-12018-OFI_M, 10-08-00941a, 11-02-01202-a, 11-07-00273-a, 11-08-01165-a and 11-08-00457-a).

References

1. E.D. Diebold, P. Peng, E. Mazur, J. Am. Chem. Soc. **131**, 16356 (2009)
2. E.D. Diebold, N.H. Mack, S.K. Doorn, E. Mazur, Langmuir **25**, 1790 (2009)
3. Z. Huang, J.E. Carey, M. Liu, X. Guo, E. Mazur, J.C. Campbell, Appl. Phys. Lett. **89**, 033506 (2006)
4. R.A. Myers, R. Farrell, A. Karger, J.E. Carey, E. Mazur, Appl. Opt. **45**, 8825 (2006)
5. Y. Dong, P. Molian, Appl. Phys. Lett. **84**, 10 (2004)
6. S.I. Dolgaev, S.V. Lavrishev, A.A. Lyalin, A.V. Simakin, V.V. Voronov, G.A. Shafeev, Appl. Phys. A **73**, 177 (2001)
7. A.J. Pedraza, J.D. Fowlkes, Y.-F. Guan, Appl. Phys. A **77**, 277 (2003)
8. M.Y. Shen, C.H. Crouch, J.E. Carey, E. Mazur, Appl. Phys. Lett. **85**, 5694 (2004)
9. E.V. Golosov, V.I. Emel'yanov, A.A. Ionin, Yu.R. Kolobov, S.I. Kudryashov, A.E. Ligachev, Yu.N. Novoselov, L.V. Seleznev, D.V. Sinitsyn, JETP Lett. **90**, 107 (2009)
10. S.M. Klimentov, T.V. Kononenko, P.A. Pivovarov, V.I. Konov, A.M. Prokhorov, D. Breitling, F. Dausinger, Quantum Electron. **32**, 433 (2002)
11. A.A. Ionin, S.I. Kudryashov, S.V. Makarov, L.V. Seleznev, D.V. Sinitsyn, JETP Lett. **90**, 423 (2009)
12. J.E. Sipe, J.F. Young, J.S. Preston, H.M. van Driel, Phys. Rev. B **27**, 1141 (1983)
13. S.A. Akhmanov, V.I. Emel'yanov, N.I. Koroteev, V.N. Seminogov, Usp. Fiz. Nauk **147**, 675 (1985) [Sov. Phys. Usp. 28, 1084 (1985)]
14. S.I. Kudryashov, V.I. Emel'yanov, J. Exp. Theor. Phys. **94**, 94 (2002)
15. I.S. Grigor'ev, E.Z. Meylikhova (eds.), *Fizicheskie Velichini* (Energoatomizdat, Moscow, 1991)
16. B.R. Tull, J.E. Carey, E. Mazur, J. McDonald, S.M. Jalisove, Mater. Res. Soc. Bull. **31**, 626 (2006)
17. S. Jesse, A.J. Pedraza, J.D. Fowlkes, J.D. Budai, J. Mater. Res. **17**, 1002 (2002)